

RESEARCH ARTICLE

Characterization of ST14A Cells for Studying Modulation of Voltage-Gated Calcium Channels

Mandy L. Roberts-Crowley, Ann R. Rittenhouse^{1*}

Department of Physiology, Program in Neuroscience, University of Massachusetts Medical School, Worcester, Massachusetts, United States of America

¹ Current address: Department of Microbiology and Physiological Systems, Program in Neuroscience, University of Massachusetts Medical School, Worcester, MA, United States of America

* Ann.Rittenhouse@umassmed.edu



OPEN ACCESS

Citation: Roberts-Crowley ML, Rittenhouse AR (2015) Characterization of ST14A Cells for Studying Modulation of Voltage-Gated Calcium Channels. PLoS ONE 10(7): e0132469. doi:10.1371/journal.pone.0132469

Editor: Kevin P.M. Currie, Vanderbilt University Medical Center, UNITED STATES

Received: February 25, 2015

Accepted: June 15, 2015

Published: July 6, 2015

Copyright: © 2015 Roberts-Crowley, Rittenhouse. This is an open access article distributed under the terms of the [Creative Commons Attribution License](http://creativecommons.org/licenses/by/4.0/), which permits unrestricted use, distribution, and reproduction in any medium, provided the original author and source are credited.

Data Availability Statement: All relevant data are within the paper.

Funding: This work was supported by National Institute of Health (<http://www.nih.gov>) grant #R01-NS34195, and American Heart Association (<http://www.heart.org/HEARTORG/>) grant #9940225N, and funding from the University of Massachusetts Medical School (umassmed.edu) to ARR. Also the National Institute of Health Ruth L. Kirschstein National Research Service Award (NRSA) (<http://grants.nih.gov/training/nrsa.htm>) grant #5 TS32 NS07366-09 to MLR. The funders had no role in study design, data

Abstract

In medium spiny neurons (MSNs) of the striatum, dopamine D₂ receptors (D₂Rs) specifically inhibit the Ca_v1.3 subtype of L-type Ca²⁺ channels (LTCs). MSNs are heterogeneous in their expression of dopamine receptors making the study of D₂R pathways difficult in primary neurons. Here, we employed the ST14A cell line, derived from embryonic striatum and characterized to have properties of MSNs, to study Ca_v1.3 current and its modulation by neurotransmitters. Round, undifferentiated ST14A cells exhibited little to no endogenous Ca²⁺ current while differentiated ST14A cells expressed endogenous Ca²⁺ current. Transfection with LTC subunits produced functional Ca_v1.3 current from round cells, providing a homogeneous model system compared to native MSNs for studying D₂R pathways. However, neither endogenous nor recombinant Ca_v1.3 current was modulated by the D₂R agonist quinpirole. We confirmed D₂R expression in ST14A cells and also detected D₁Rs, D₄Rs, D₅Rs, G_q, calcineurin and phospholipase A₂ using RT-PCR and/or Western blot analysis. Phospholipase C β-1 (PLCβ-1) expression was not detected by Western blot analysis which may account for the lack of LTC modulation by D₂Rs. These findings raise caution about the assumption that the presence of G-protein coupled receptors in cell lines indicates the presence of complete signaling cascades. However, exogenous arachidonic acid inhibited recombinant Ca_v1.3 current indicating that channels expressed in ST14A cells are capable of modulation since they respond to a known signaling molecule downstream of D₂Rs. Thus, ST14A cells provide a MSN-like cell line for studying channel modulation and signaling pathways that do not involve activation of PLCβ-1.

Introduction

Two classes of L-type Ca²⁺ channel (LTC) α₁ subunits are expressed in the brain: α_{1C} (Ca_v1.2) and α_{1D} (Ca_v1.3) [1] with highest expression in cerebral cortex and striatum [2]. While differing in biophysical properties and pharmacological sensitivities, both LTCs contribute to

collection and analysis, decision to publish, or preparation of the manuscript.

Competing Interests: The authors have declared that no competing interests exist.

membrane excitability, synaptic regulation and gene transcription [3]. In turn, neurotransmitters act via G-protein coupled receptors (GPCRs) to modulate membrane excitability and alter transfer of information within neural circuits. Modulation of LTCs by dopamine GPCR signaling pathways is important in medium spiny neurons (MSN) of the striatum since these neurons are the only source of output from the striatum [4] and are adversely affected in both Parkinson's and Huntington's Diseases [5, 6].

Two families of dopamine receptors exist. The D₁-like receptor family (D₁R, D₅R), couples to the G protein G_s, enhancing L-current [7, 8] and the firing rate of MSNs [7]. Conversely, the D₂-like receptor family (D₂R, D₃R, D₄R) couples to G_{i/o} [9], inhibiting L-current [10] and the firing rate of MSNs [11]. Two heterogeneous groups of MSNs respond to dopaminergic input: D₁R-expressing MSNs and D₂R-expressing MSNs, which are associated with the direct and indirect output, respectively [6]. The balance of output pathways between the opposing D₁R- and D₂R-expressing MSNs coordinates motor control [12]. Consequently drugs developed to treat Parkinson's disease target dopamine receptors, particularly D₂Rs [13] and more recently LTCs [14, 15]. MSNs express both Ca_v1.2 and Ca_v1.3, but D₂R activation inhibits only Ca_v1.3 [11]. In Parkinson's disease models, loss of D₂R modulation of Ca_v1.3 leads to loss of dendritic spines [16]. Therefore, the pathway underlying D₂R modulation of LTC current appears critical for normal function; however due to dopamine receptor heterogeneity in MSNs, the molecular relationship between D₂Rs and LTCs has been difficult to elucidate.

Moreover, two different mechanisms may mediate D₂R inhibition of LTC current. One characterized pathway involves G_q, phospholipase C (PLC), inositol triphosphate (IP₃)-induced Ca²⁺ release, and protein phosphatase 2B (PP2B) also known as calcineurin [10]. Additionally, D₂R activation releases arachidonic acid (AA) *in vivo* [17–20], in primary neurons [21] and in transfected cell lines [22]. Our laboratory has demonstrated that exogenously applied AA inhibits LTC currents in superior cervical ganglion neurons (SCG) [23–25]. These currents are most likely exclusively due to Ca_v1.3 current [26]. Additionally, we have shown that AA inhibits recombinant Ca_v1.3 currents when expressed in HEK293 cells [27]. Therefore, a second D₂R signaling pathway inhibiting Ca_v1.3 may involve activation of Ca²⁺-dependent cytosolic phospholipase A₂ (cPLA₂), which cleaves AA from phospholipids, similar to M₁ muscarinic receptor (M₁R) modulation of LTC current in SCG [25].

In the present study, we developed a model system to probe the D₂R signaling pathway inhibiting Ca_v1.3 using the ST14A cell line, created from embryonic rat striatum [28]. Retroviral transduction of the temperature-sensitive SV40 large T antigen enables ST14A cells to grow and divide at the permissive temperature of 33°C. At higher temperatures the cells differentiate to exhibit general neuronal, as well as specific MSN-like, properties including functional D₂-like receptors [28, 29]. We examined whether ST14A cells express identified signaling molecules downstream of D₂Rs in an effort to develop a model cell line with MSN properties to study the functional effects of D₂R signaling on Ca_v1.3. We found that round ST14A cells lacked endogenous Ca²⁺ current and exploited this deficiency by transfecting cells with Ca_v1.3 and accessory subunits, thus eliminating the need for pharmacological blockers. Recombinant Ca_v1.3 currents were characterized and tested for current modulation by the D₂ dopamine agonist quinpirole and by exogenous AA.

Materials and Methods

Preparation of Cells

The ST14A cell line, created by Elena Cattaneo and described in Cattaneo and Conti, 1998 [28], was given to us as a gift from Dr. Michelle E. Ehrlich (Jefferson Medical School) with permission from Dr. Elena Cattaneo (University of Milano). ST14A cells were propagated at the

permissive temperature of 33°C in Dulbecco's modified Eagle's medium (DMEM; Gibco) supplemented with 0.11 g/L sodium bicarbonate (Sigma, St. Louis, MO), 0.29 g/L L-glutamine, 3.9 g/liter HEPES, 100 units/ml penicillin-streptomycin, and 10% fetal bovine serum (FBS; Invitrogen, Carlsbad, CA). Cells were transferred to 37°C to promote differentiation and used 1–2 days later. The A9L cell line, derived from A9 L cells co-transfected with the human D₂R and obtained from the American Type Culture Collection (ATCC, Manassas, VA), were propagated at 37°C in DMEM with 4 mM L-glutamine adjusted to contain 1.5 g/L sodium bicarbonate and 4.5 g/L glucose containing 10% FBS. HEK 293 cells were propagated at 37°C in DMEM/F12 containing 10% FBS. All cells were maintained in a temperature-controlled humidified incubator at 5% CO₂ and passaged once flasks became 80–90% confluent. SCG, striatum and cortex of 1 to 4-day old or adult Sprague-Dawley rats (Charles River Laboratories, Wilmington, MA) were isolated following CO₂ exposure and decapitation using a protocol (protocol # 822) approved by the Institutional Animal Care and Use Committee (IACUC) of University of Massachusetts Medical School. This study was carried out in strict accordance with the recommendations in the Guide for the Care and Use of Laboratory Animals of the National Institutes of Health. All efforts were made to minimize animal suffering. The Institutional Animal Care and Use Committee (IACUC) of University of Massachusetts Medical School specifically approved animal use for this study.

Electrophysiology

Whole-cell currents were recorded at room temperature (RT, 20–24°C) with an Axon 200B patch clamp amplifier (Molecular Devices, Sunnyvale, CA). Currents were filtered at 1–5 kHz and digitized at 5 times the filter cut-off frequency of the 4-pole Bessel filter of the amplifier. Electrodes were pulled from borosilicate glass capillary tubes and each electrode was fire-polished to ~1 m to give the pipette a resistance of 2–3 M. The pipette solution consisted of (in mM): 125 Cs-Aspartate, 10 HEPES, 0.1 BAPTA, 5 MgCl₂, 4 ATP and 0.4 GTP brought to pH 7.50 with CsOH. High resistance seals were established in Ca²⁺ Tyrode's consisting of (in mM): 5 CaCl₂, 145 NaCl, 5.4 KCl, and 10 HEPES brought to pH 7.50 with NaOH. Once a seal was established and the membrane ruptured, the Tyrode's solution was exchanged for an external bath solution consisting of (in mM): 125 NMG-Aspartate, 20 Ba²⁺, 10 HEPES brought to pH 7.50 with CsOH.

FPL 64176 and nimodipine were prepared as stock solutions in 100% ethanol and stored at -20°C. AA (5,8,11,14-eicosatetraenoic acid; NuCheck Prep, Elysian, MN) and oleic acid (NuCheck Prep) were dissolved in 100% ethanol and stored under nitrogen as stock solutions at -70°C. ω -conotoxin GVIA (Bachem, Torrance, CA) and quinpirole were prepared as stock solutions in double distilled water and stored at -70°C. Oxotremorine-M (Tocris, Ellisville, MO) was prepared fresh daily by making a 10 mM stock in double distilled water. Working dilutions were made fresh daily by diluting stock solutions at least 1:1,000 with external bath solution. For ethanol prepared stocks, the final ethanol concentration was less than 0.1%. Bovine serum albumin (BSA; fraction V, heat shock, fatty acid ultra-free; Roche Applied Science, Indianapolis, IN) was added directly to the bath solution for a final concentration of 1 mg/ml. All chemicals were purchased from Sigma unless otherwise noted.

Data were acquired using Signal 2.14 software (Cambridge Electronic Design, Cambridge, England) and stored for later analysis on a personal computer. Linear leak and capacitive currents were subtracted from all traces. Data are presented as the mean \pm s.e.m. Significance was determined statistically using a two-tailed paired or unpaired *t*-test, or a one-way ANOVA. Analysis programs include Signal (Cambridge Electronic Design), Excel (Microsoft, Redmond, WA) and Origin (OriginLab, Northampton, MA).

Transfection

ST14A cells were transfected by lipofectamine (Invitrogen, Carlsbad, CA) with a 1:1:1 molar ratio of Ca_v1.3, β_{2a}, and α_{2δ} subunits [30]. Constructs for Ca_v1.3b (+exon11, Δexon32, +exon42a; GenBank accession #AF370009), and α_{2δ}-1 (GenBank accession #AF286488) were a gift from Dr. Diane Lipscombe (Brown University) and the construct for Ca_vβ_{2a} (GenBank accession #M80545) was a gift from Dr. Edward Perez-Reyes (University of Virginia). For all transfections, 0.4 μg of DNA was used per well of a 12-well plate. Prior to transfection, cells were washed with DMEM. The DNA mixture was then added dropwise to each well, gently swirled then incubated for 1–3 h at 37°C in a 5% CO₂ incubator. Supplemented media, without antibiotics, was returned to the wells to bring the volume up to 1 ml (normal growth medium volume). Cells were washed with full media 2 and 4 h later and assayed for transient gene expression after 24–72 h.

Reverse Transcriptase-Polymerase Chain Reaction

Homogenized tissue samples (50–100 mg) or confluent cells in a 100 mm dish were lysed in 1 ml TRIzol Reagent (Invitrogen). RNA was separated from DNA by phenol-chloroform phase separation. RNA was precipitated with isopropyl alcohol and washed with 75% ethanol. The RNA pellet was dried and resuspended in RNase-free water. RNA samples had an A₂₆₀/A₂₈₀ ratio between 1.6 and 1.8 and were treated with DNase to eliminate contamination with genomic DNA. For reverse transcription, cDNA was synthesized from the mRNA by adding 1 μl 10X buffer RT, 1 μl dNTP Mix (5 mM each dNTP), 1 μl Oligo-dT primer (0.5 mg/ml, Promega, Madison, WI), 0.125 μl RNase Inhibitor (40 U/μl, Promega), 0.5 μl Omniscript Reverse Transcriptase (4 U/μl) and RNase-free water for a total volume of 10 μl (all reagents from QIAGEN, Valencia, CA, unless otherwise noted). The mixture was incubated at 37°C for 1 h. The mixture was then heated at 93°C for 5 min and then placed on ice to inactivate the transcriptase. PCR amplification was then performed with a Techgene thermal cycler (Techne Inc, Burlington, NJ) with thin walled PCR tubes.

PCR primers for dopamine receptors D₁–D₅ (D₅ formerly referred to as D_{1b}) were sequences previously published [31]. D₁: 5′ –GAC AAC TGT GAC ACA AGG TTG AGC–3′ and 5′ –ATT ACA GTC CTT GGA GAT GGA GAT GGA GCC–3′ yields a 609 base pair (bp) product. D₂: 5′ –GCA GTC GAG CTT TCA GAG CC–3′ and 5′ –TCT GCG GCT CAT CGT CTT AAG–3′ yields 404 and 317 bp products recognizing the long and short forms of the D₂R, respectively. D₃: 5′ –AGC ATC TGC TCC ATC TCC AAC CC–3′ and 5′ –A GGA GTT CCG AGT CCT TTC CAC G–3′ yields a 461 bp product. D₄: 5′ –TC ATG CTA CTG CTT TAC TGG GCC A–3′ and 5′ –T CTG AGA GAG GTC TGA CTC TGG TC–3′ yields a 223 bp product. D₅: 5′ –AGT CGT GGA GCC TAT GAA CCT GAC–3′ and 5′ –GCG TCG TTG GAG AGA TTT GAG ACA–3′ yields a 517 bp product. GAD65 and GAD67 primers were from sequences previously published [32]. GAD65: 5′ –CGC CCC TGT ATT TGT ACT AC–3′ and 5′ –GCC AAG AGA GGA TCA AAA GC–3′ yields a 400 bp product. GAD67: 5′ CAC ACC AGT TGC TGG AAG–3′ and 5′ –ACA AAC ACG GGT GCA ATT–3′ yields 318 and 238 bp products. GAPDH primers were from sequences previously published [33]. GAPDH: 5′ –TGC CAA GGC TGT GGG CAA GG–3′ and 5′ –GCT TCA CCA CCT TCT TGA TG–3′ yields a 199 bp product and confirmed equal loading.

Reaction mixtures for PCR contained 200 ng of cDNA, 5 μl of 2.5 X Eppendorf MasterMix [Taq DNA Polymerase (62.5 U/ml), 125 mM KCl, 75 mM Tris-HCl, 3.75 mM Mg(OAc)₂, 0.25% Igepal-CA630, 500 μM of each dNTP and stabilizers, Brinkmann, Westbury, NY], 1 μl each of forward and reverse primer (5 pmol/ μl, Invitrogen for dopamine receptors and GAD; Qiagen for GAPDH), 2 to 4 mM Mg²⁺ (Brinkmann) and distilled water to a final volume of

12.5 μ l. High (4 mM) Mg²⁺ concentrations were necessary to amplify dopamine receptor mRNAs. The protocol for dopamine receptor amplification was 94°C for 1 min, 58°C for 1 min, and 72°C for 3 min for 20 cycles [31]. For the D₃R, an annealing temperature of 62°C was also tried. For GAD amplification, the protocol was 94°C for 3 min, 53°C for 1 min, 52°C for 1 min, 51°C for 1 min, and 70°C for 2 min for 30 cycles [32]. A 2 μ l aliquot was used as a template for a second round of amplification for thirty cycles. PCR products and a 100 bp DNA ladder (Invitrogen; bright band 600 bp or Promega, Madison, WI; bright band 500 bp) were separated by electrophoresis in 2% agarose gels stained with ethidium bromide. Bands excised from gels were sequenced by the UMASS Medical School Nucleic Acid Facility and compared to published sequences (GenBank accession number): D₁ (M35077), D₂ (M36831), D₄ (M84009), D₅ (M69118), GAD65 (M74826), and GAD67 (M81883).

Western Blot Analysis

The immunoblot protocol has been previously described [34]. All extracts and buffers contained protease inhibitors (Santa Cruz Biotechnology, Santa Cruz, CA): pepstatin A (1 μ g/ml), leupeptin (10 μ g/ml), aprotinin (20 μ g/ml), phenylmethanesulfonyl fluoride (200 nM), and calpain inhibitor I and II (8 μ g/ml each). Day 4 rat brain or cells grown in uncoated 60-mm dishes were solubilized in lysis buffer (0.15 M NaCl, 5 mM EDTA, 1% Triton-X 100, 10 mM Tris-Cl pH 7.4), sonicated, and centrifuged to remove insoluble material. Protein concentration was determined by the RC/DC assay (Bio-Rad, Hercules, CA). 20–30 μ g of protein was loaded per lane and separated on 8% SDS-polyacrylamide gels. Equal protein loading was confirmed by staining with β -actin antibodies.

Antibodies used include: *monoclonal*- D₂R (1:400; Santa Cruz Biotechnology), PP2B and β -actin (1:500 and 1:10,000; Sigma); *polyclonal*- M₁R and G_q α (1:1,000; Santa Cruz Biotechnology), cPLA₂ (1:200; Cell Signaling Technology, Danvers, MA), PLC β -1 (1:200; Millipore, Billerica, MA); *secondary*- HRP-conjugated goat anti-mouse or bovine anti-rabbit (1:15,000 or 1:10,000; Santa Cruz Biotechnology). Primary and secondary antibodies were diluted with PBS.

Results

To determine if ST14A cells express endogenous Ca²⁺ current, we measured whole-cell currents from cells grown at 33 or 37°C. Two populations of cells were distinguished based on morphology: round or differentiated, with the definition of having neuron-like projections. From a holding potential of -90 mV, round cells exhibited zero to little endogenous peak or tail current measured at +10 mV or -40 mV respectively, regardless of the temperature at which the cells were grown (Fig 1A). Differentiated cells had significantly more endogenous current than round cells at both potentials (Fig 1B). Application of the LTC agonist, FPL 64176 (FPL; 1 μ M) enhanced endogenous currents at both potentials (Fig 1A and 1B), indicating that at least a component of the endogenous current was LTC. Since round cells showed little to no LTC current, we transfected the ST14A cells with LTC channel subunits, Ca_v1.3, β_{2a} , and $\alpha_2\delta$ -1, along with green fluorescent protein (GFP) and recorded whole-cell currents from green fluorescing round cells (Fig 1C). Peak and tail currents from round transfected cells were significantly larger than those recorded from round untransfected cells (Fig 1A and 1B). FPL significantly enhanced recombinant current at -40 mV. Fig 1D shows representative individual traces of round endogenous or round recombinant current before and after application of FPL. The recombinant current shows little to no inactivation with 20 mM Ba²⁺ as the charge carrier [35], typical of LTC current coexpressed with the accessory subunit, β_{2a} [36].

Since Ca_v1.3 activates at more negative voltages compared to Ca_v1.2 [30], we measured peak current at -10 mV. Recombinant current recorded at -10 mV was larger than at +10 mV

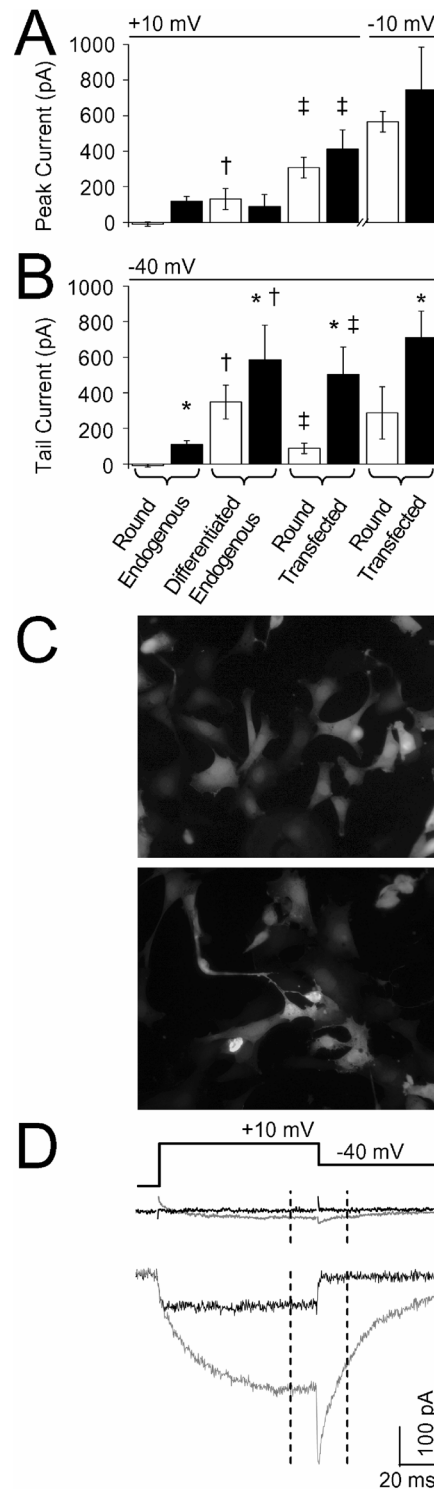


Fig 1. ST14A cells have endogenous Ca²⁺ currents but are capable of expressing recombinant current. (A-B) Currents were recorded from round (undifferentiated, no processes) or differentiated (having processes) endogenous ST14A cells. Note: round cells from ST14A cells grown at either 33°C or 37°C exhibited little to no current and were pooled. Currents were recorded from round ST14A cells grown at 33°C, transfected and grown at 37°C for at least 24 hours before recording. Each set of cells were recorded in the absence (white bars) and presence of 1 μM FPL (black bars). Summary of peak Ca²⁺ currents measured from a holding potential of -90 mV to a test potential of +10 mV (A) and then to a tail potential of -40 mV (B).

Endogenous current from differentiated cells was significantly larger than endogenous current from round cells (\dagger ; $p < 0.05$); Transfected current was significantly larger than endogenous current from round cells (\ddagger ; $p < 0.05$); FPL significantly increased differentiated endogenous and transfected tail current ($*$; $p < 0.05$), $n = 7-15$. (C) Transfected ST14A cells expressed GFP throughout the cell soma and in a small percentage of differentiated cells, in the processes. Images (20X magnification) were captured ~24 hours post-transfection. The transfection rate for these cells was ~50%. (D) *Top*: Protocol for eliciting currents from a holding potential of -90 mV to the test potential of +10 mV for 100 ms before repolarizing to -40 ms. Individual traces from round endogenous (*middle*) or round transfected (*bottom*) cells. Dashed lines indicate where peak and tail current were measured 65 ms after depolarization and 15 ms after repolarization, respectively. In the presence of LTC agonist, 1 μ M FPL, both the peak and long-lasting tail current increase (gray trace) and display slowed activation and deactivation kinetics, characteristic of FPL-induced L-current.

doi:10.1371/journal.pone.0132469.g001

(Fig 1A) and this increase was also reflected in the tail current amplitude at -40 mV (Fig 1B). The summary of these results shows that round ST14A cells have little endogenous LTC current but are capable of being transfected with LTCs and expressing functional LTC currents. Therefore, the round cells represent a population of ST14A cells that we used to study recombinant LTC function in isolation from other types of native Ca²⁺ channels.

We characterized recombinant Ca_v1.3 current further to determine whether transfected channel activity in ST14A cells exhibits biophysical and pharmacological properties of Ca_v1.3 observed in oocytes and HEK 293 cells [30]. First, we measured peak current across a range of voltages to show that channels open at relatively negative voltages compared to Ca_v1.2 [30]. Indeed, in 20 mM Ba²⁺, Ca_v1.3 currents activated at a test potential of -60 mV and peaked at -10 mV to 0 mV (Fig 2A). Recombinant current in ST14A cells exhibited a Ca_v1.3 LTC pharmacological profile. Fig 2B shows a time course of the effects of Ca²⁺ channel ligands on Ca_v1.3 current. The current was insensitive to the N-type Ca²⁺ channel antagonist, ω -conotoxin GVIA (1 μ M; CTX) but was inhibited in a concentration-dependent manner by the LTC antagonist, nimodipine (0.1–3.0 μ M; NIM). The inhibition produced by 1.0 μ M NIM (51.8 \pm 4%) is characteristic of the low-voltage sensitivity of Ca_v1.3 compared to Ca_v1.2, which would be fully blocked by 1.0 μ M NIM [30]. Inhibition fully reversed by washing with bath solution. After wash out, channels remained sensitive to FPL. The antagonist data are summarized in the bar graph in Fig 2C. These findings show that recombinant current in ST14A cells displayed both current-voltage and pharmacological profiles specific to Ca_v1.3 channels.

To determine whether D₂R activation by the agonist quinpirole (Quin) inhibits Ca_v1.3 currents in ST14A cells, we recorded recombinant currents in the presence of FPL to enhance current amplitude. At a concentration of 10 μ M, Quin had no significant effect on peak or tail current amplitude over time, (Fig 3A left) or in individual traces (Fig 3A right). To determine if only recombinant Ca_v1.3 current was insensitive to D₂R activation, we tested whether endogenous ST14A current from differentiated cells could undergo modulation. Again 10 μ M Quin had no significant effect on endogenous peak or long-lasting tail current amplitude. Fig 3B shows representative current traces in the presence of 1 μ M FPL from a range of voltages before and after Quin. Since a majority of MSNs express muscarinic M₁ receptors (M₁Rs) as well as dopamine receptors [37], we tested whether activation of this receptor would inhibit endogenous current. The muscarinic agonist oxotremorine-M (Oxo-M; 10 μ M) had no effect on endogenous peak or long-lasting tail current amplitude. Fig 3C shows representative current traces in the presence of FPL from a range of voltages (-60 mV to -10 mV) tested before and after Oxo-M. Fig 3D summarizes the effect of Quin and Oxo-M on peak (left) and long-lasting tail current (right) from recombinant Ca_v1.3 versus endogenous ST14A current. These results suggest that the D₂R and M₁R signaling pathways, which inhibit LTC current in MSNs, are not intact in ST14A cells. However, application of dopamine or Quin, increases CREB

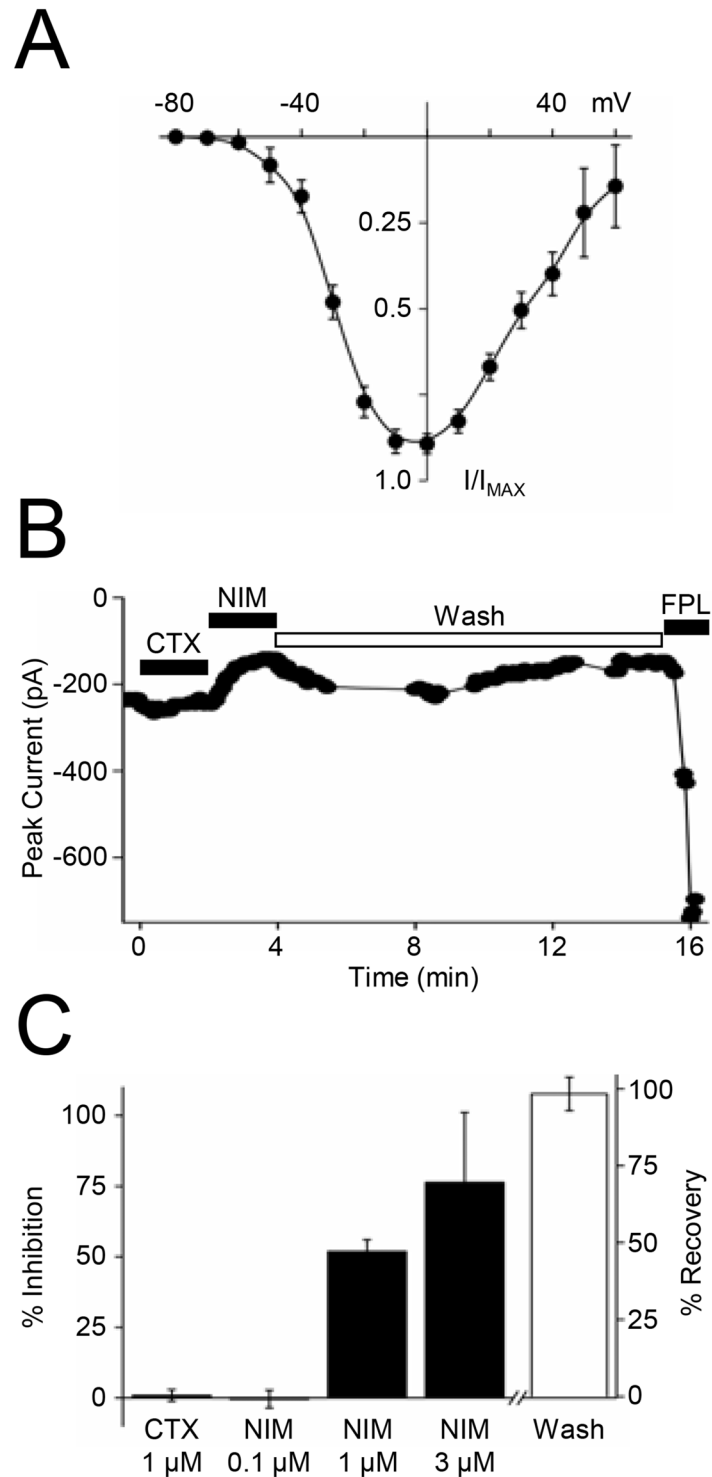


Fig 2. Whole-cell currents from transfected ST14A cells have biophysical and pharmacological properties of Ca_v1.3 LTCs. (A) The current-voltage (I-V) relationship shows that recombinant Ca_v1.3 current activates at approximately -60 mV; n = 15. (B) Example time course of peak current at -10 mV. 1 μ M ω -conotoxin GVIA (CTX, an N-type Ca²⁺ channel antagonist) was added for 2 min. Bath solution was exchanged with 1 μ M nimodipine (NIM, an LTC antagonist) for 2 min or until a new stable baseline was reached and then washed off to show reversibility. FPL (1 μ M) was added at the end of the recording. (C) Summary of pharmacological inhibition of transfected current; n = 3–6.

doi:10.1371/journal.pone.0132469.g002

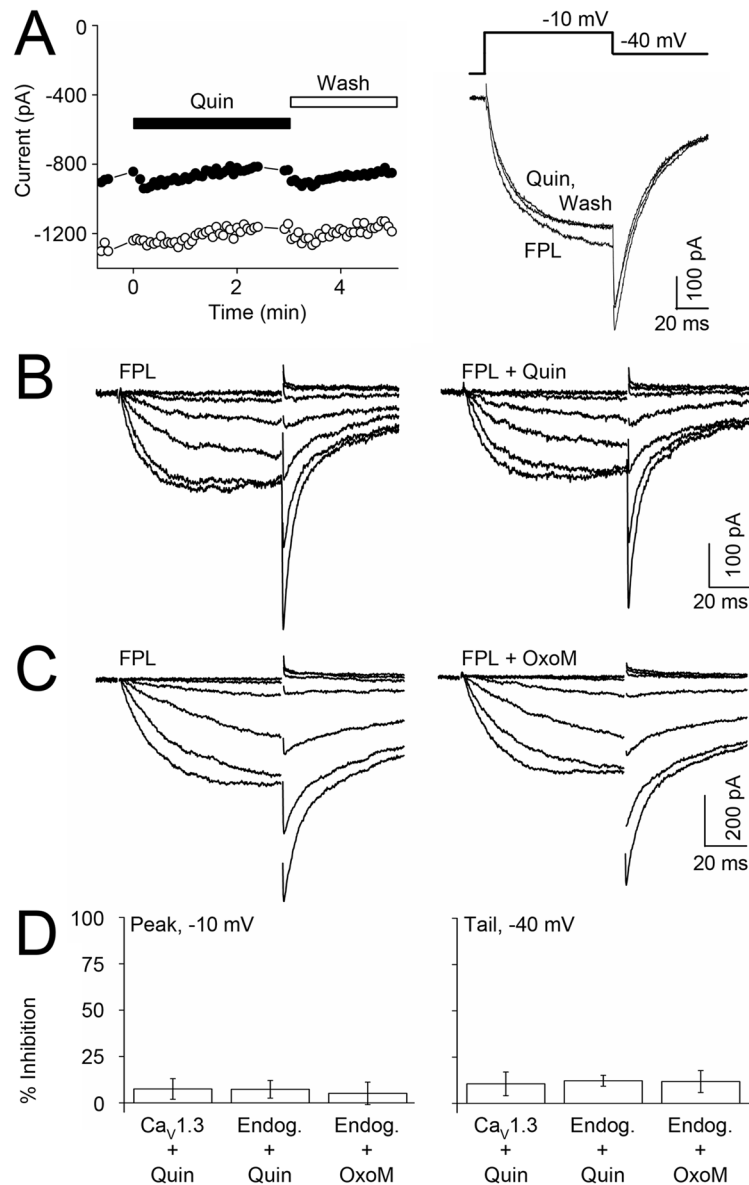


Fig 3. ST14A endogenous or recombinant Ca_v1.3 current is not modulated by GPCR activation. (A) Time course (left) and representative sweeps (right) of recombinant Ca_v1.3 current before (FPL), 1 min following 10 μM quinpirole application (Quin) and after removing Quin (Wash). (B–C) Endogenous, differentiated current traces in the presence of FPL across a range of test potentials (-50 mV to 0 mV) before (left) and after (right) application of (B) 10 μM Quin or (C) 10 μM oxotremorine M (Oxo-M). (D) Summary of percent inhibition of peak (left) and long-lasting tail (right) recombinant Ca_v1.3 or endogenous currents by D₂R or M₁R agonist; n = 3–7.

doi:10.1371/journal.pone.0132469.g003

phosphorylation in ST14A cells, indicating that D₂Rs do couple to intact signaling cascades such as the adenylyl cyclase and MAPK pathways [29].

A non-selective D₂R-like agonist, Quin also activates D₃ and D₄Rs [38]. Subsequently, D₃ and D₄Rs modulate immediate early gene expression [39, 40] raising the question of the identity of dopamine receptors in ST14A cells. Using RT-PCR, we examined dopamine receptor (D₁, D₂, D₃, D₄, and D₅) mRNA content in ST14A cells, striatum (positive control for all dopamine receptors), cortex, A9L cells (D₂R positive control; see [Materials and Methods](#)) or HEK

293 cells (negative control for all dopamine receptors). PCR products were detected for long and short splice variants of the D₂R in ST14A cells (n = 4/11 and 2/11, respectively, striatum (n = 1/2 and 2/2, respectively), cortex (n = 1/2 for both) and A9L cells (n = 2/5 and 2/5, respectively) as shown in Fig 4A. Additionally, D₁R (n = 2/10), D₄R (7/10), D₅R (4/10) (data not shown) mRNAs were also detected in ST14A cells, regardless of the temperature at which cells were grown. D₁R, D₄R and D₅R mRNAs were detected in striatum whereas D₁R and D₄R mRNAs were detected in the cortex (data not shown). D₄R mRNA was also detected in A9L cells (n = 3/4). Experiments for D₃R mRNA expression in striatum, cortex, and ST14A cell samples resulted in a smear despite several attempts to adjust the protocol. HEK 293 cells showed no expression of any of the dopamine receptors tested. These results show that ST14A cells express mRNA for more than one D₂-like receptor; this finding could account for the previously reported D₂R-like changes in pCREB [29].

Since MSNs are GABAergic, a defining characteristic of ST14A cells being MSN-like would be expression of glutamic acid decarboxylase (GAD), the enzyme that catalyzes GABA synthesis from glutamate. Using RT-PCR, we measured whether ST14A cells express GAD2 and GAD1, two genes which encode GAD with molecular weights of 65 and 67 kDa, respectively. The primers used against GAD1 detect both embryonic and adult splice forms of GAD67. All three bands corresponding to GAD65 and embryonic and adult GAD67 were detected in ST14A cells (Fig 4B). Alternate lanes in which RNA samples were not reverse transcribed served as controls for genomic DNA contamination and yielded no product. Using striatal and cortical tissues as positive controls for the GAD genes, and in A9L cells, we detected all three forms of GAD as well. In contrast, no bands for GAD65 and only faint bands for GAD67 were detected in HEK 293 cells. The presence of GAD in ST14A cells further confirms that this cell line exhibits GABAergic characteristics of MSNs.

After confirming ST14A cells exhibit a similar mRNA expression profile for dopamine receptors and GAD as MSNs, we examined whether D₂Rs and downstream signaling molecules were expressed in ST14A cells. Using Western blot analysis, D₂R and M₁R expression was confirmed in ST14A cells. D₂R antibodies recognized a band at 50 kDa, the expected molecular weight of D₂Rs (Fig 5A, top panel) for striatum and cortex (positive controls). A second band at 75 kDa, absent in the A9L cell line, most likely represents a glycosylated form of the receptor [41], further supporting the idea that the ST14A cells are similar to neurons in these brain regions regarding post-translational modification of proteins. Fig 5A (middle panel) shows that ST14A cells, but not A9L cells, express M₁Rs, displayed as a 50 kDa band on Western blots. This antibody recognized M₁R expression in SCG, striatum, and cortex [34]. Expression of G_qα (Fig 5A, bottom panel), which couples to M₁Rs, was also detected in the cell lines and tissue samples at the predicted molecular weight of 42 kDa. These results show that ST14A cells express D₂R, M₁R and G_qα proteins.

Since D₂Rs and M₁Rs both couple to PLCβ-1, we examined whether ST14A cells express PLCβ-1. Protein expression of PLCβ-1 was not detected in either the A9L or ST14A cell lines, but was detected in SCG tissue (Fig 5B). The unanticipated absence of PLCβ-1 may account for the lack of Ca_v1.3 modulation since PLCβ-1 is required for LTC current inhibition by both the D₂R and M₁R pathways [10, 42]. To determine the presence of molecules downstream of PLCβ-1 reported to participate in LTC modulation by these receptors [10, 25], we tested for cPLA₂ and PP2B expression. Fig 5C shows that ST14A cells cultured at 33 and 37°C, as well as A9L cells, express cPLA₂. cPLA₂ was detected at low expression levels from postnatal day 1 SCG (positive control) as has been reported previously [25]. Fig 5D shows that ST14A cells also express PP2B. Since PLCβ-1 is downstream of both D₂ and M₁Rs, this result may explain our lack of inhibition of Ca_v1.3 or endogenous LTC current by Quin or Oxo-M in ST14A cells.

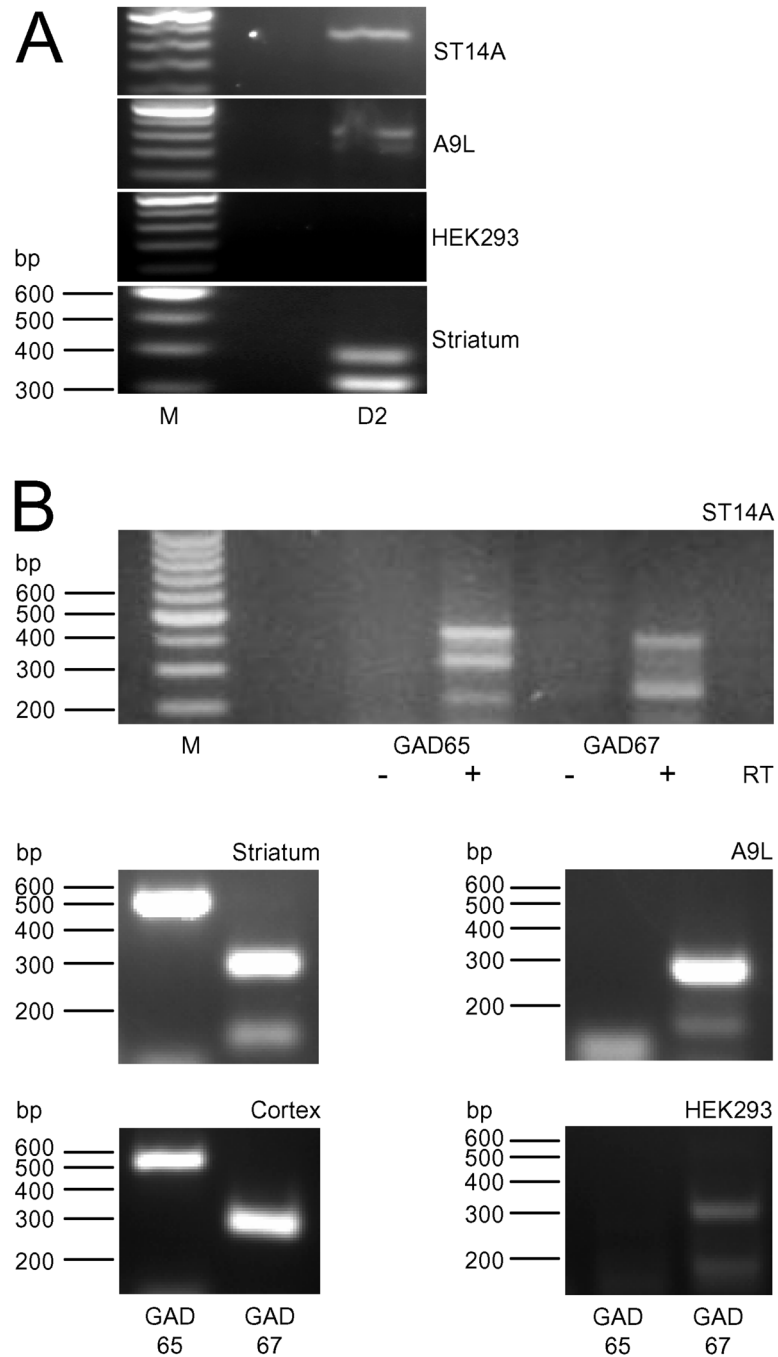


Fig 4. ST14A cells express several D₂R family mRNAs. ST14A mRNA transcripts were amplified by RT-PCR. (A) D₂R mRNA expression in ST14A, A9L, HEK 293 cells and in striatum. A9L cells that express D₂R and striatum served as positive controls. Left lane contains a 100 bp ladder; brightest band is 600 bp. The band for ST14A cells was sequenced and BLAST search results matched previously published sequences for D₂R. No D₂R bands were detected in HEK 293 cells. (B) GAD65/67 mRNA expression in ST14A, striatum, cortex, A9L and HEK 293 cells. As a control, ST14A mRNA was not reverse-transcribed (-RT).

doi:10.1371/journal.pone.0132469.g004

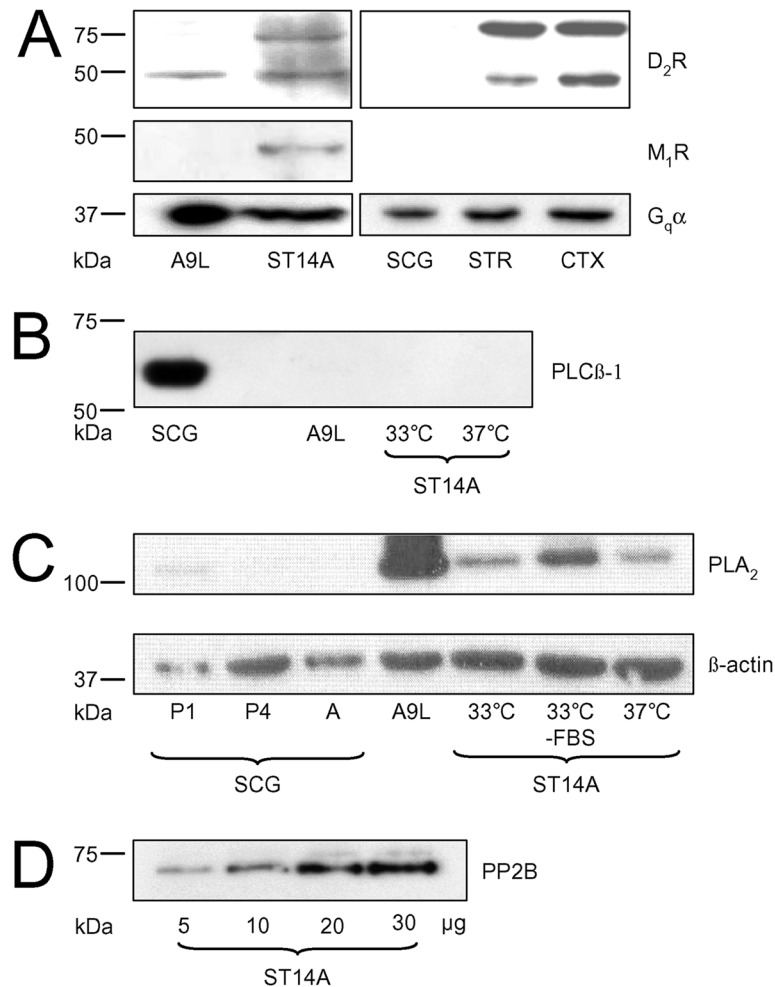


Fig 5. Expression of D₂R and M₁R signaling pathway proteins in ST14A cells. (A) *Top*: D₂R expression in ST14A cells, A9L cells (positive control) and tissues: SCG (superior cervical ganglia), STR (striatum, positive control), CTX (cortex). The predicted molecular weight (MW) for the D₂R is 50 kDa. The 75 kDa form may represent a glycosylated form of the D₂R versus long and short D₂R splice variants, which differ by ~40 amino acids and would not account for this MW difference. *Middle*: M₁R expression in ST14A or A9L cells. The predicted MW of M₁R is 50 kDa. *Bottom*: G_qα expression in both cell lines and brain tissues. The predicted MW for G_qα is 42 kDa. (B) PLCβ-1 expression, or absence, in SCG, A9L or ST14A cells at various temperatures. The antibody recognizes PLCβ-1 fragments at 100 and 41 kDa. (M, lane for MW ladder) (C) The presence of cPLA₂ in SCG neurons at postnatal day 1 (P1) or 4 (P4) or adult (A), A9L and ST14A cells under varying conditions. The predicted MW for cPLA₂ is 110 kDa. β-actin, MW of 42 kDa, is shown as a loading control. (D) PP2B in ST14A cells loaded at varying concentrations; predicted MW of the α-subunit is 61 kDa.

doi:10.1371/journal.pone.0132469.g005

To circumvent the absence of a key signaling molecule, and determine whether Ca_v1.3 could be modulated, we directly applied exogenous AA (10 μM) to the bath and measured Ca_v1.3 recombinant current over several minutes. In the presence of FPL, AA inhibited Ca_v1.3 peak and long-lasting tail currents by 40 ± 12% and 29 ± 25% respectively after 1 min (n = 4). Fig 6A shows representative sweeps before (FPL) and after AA application (FPL + AA). The large variability in tail current inhibition by AA suggested that voltage may be important for this modulation. However, AA inhibited Ca_v1.3 current at all voltages when tested over a range of test potentials as shown in the I-V plot in Fig 6B. Bovine serum albumin (BSA), which binds free fatty acids [43], reversed inhibition at all test potentials. To show that inhibition was

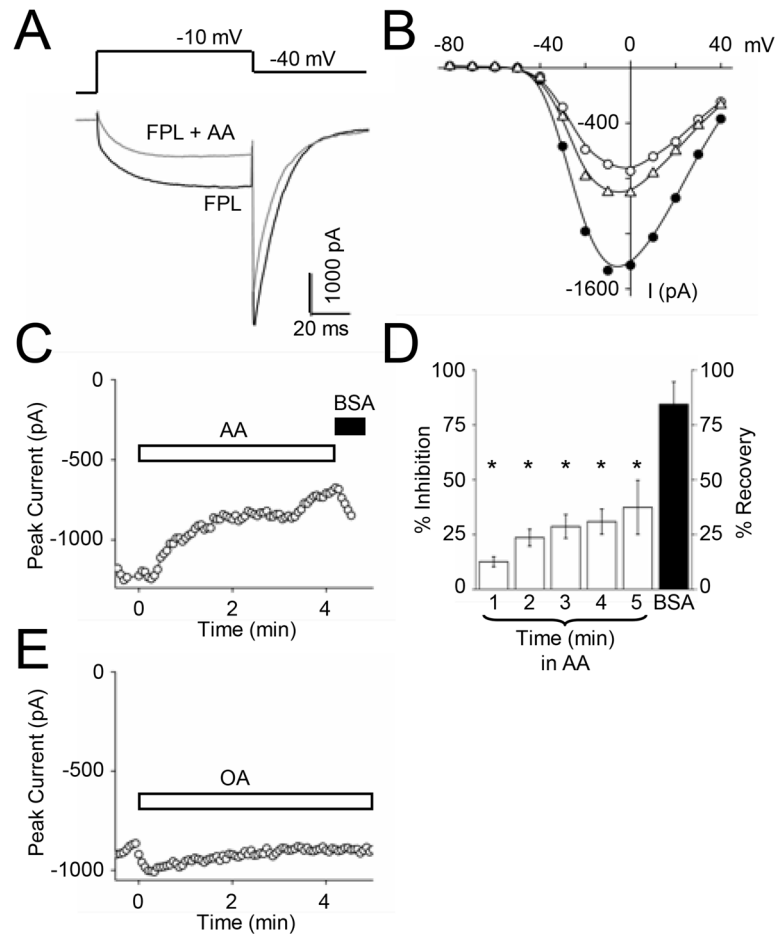


Fig 6. Transfected Ca_v1.3 currents in ST14A cells are inhibited by AA. (A) Individual sweeps with 1 μM FPL (black trace), and 1 min after 10 μM AA (dotted trace) in the continued presence of FPL. AA inhibited both peak and tail currents; n = 4. (B) I-V relationship of recombinant current in the presence of FPL (●), FPL + AA (○), and after washing off AA with bath solution containing FPL (Δ). (C) Time course of Ca_v1.3 current at -10 mV with 10 μM AA. After 4 min, AA was washed off with 1 mg/ml BSA. (D) Summary of Ca_v1.3 current inhibition by AA over time (open bars) and its recovery following BSA (Black bar); *p < 0.001; n = 5–7. (E) Time course of peak Ca_v1.3 current with 10 μM oleic acid (OA); n = 3.

doi:10.1371/journal.pone.0132469.g006

not due to AA competing with FPL, we measured Ca_v1.3 current in the absence of FPL prior to and after application of AA (Fig 6C) and still observed inhibition that could be reversed after adding BSA. Inhibition of Ca_v1.3 over time by AA (open bars) and recovery by BSA (solid bar) is summarized in Fig 6D. Conversely, oleic acid (10 μM) enhanced current by 7.9 ± 0.7% after 1 minute (Fig 6E; p < 0.001; n = 3), suggesting that inhibition by AA is not simply the result of a nonspecific fatty acid effect. Moreover, inhibition of Ca_v1.3 by AA demonstrates that the transfected Ca_v1.3 LTCs in ST14A cells are capable of modulation.

Discussion

MSNs have a resting membrane potential that oscillates between ~ -85 mV (during the “down” state) and ~ -60 mV (during the “up” state) [4, 6]. Inhibition of Ca_v1.3 is of particular interest in MSNs because it activates at potentials approximately 25 mV more negative than Ca_v1.2, [30]. Since Ca_v1.3 activates at the low voltage of -60 mV, this channel may open during the “up” state and contribute to reaching threshold for firing an action potential [4]. Moreover,

increased D₂R signaling or inhibition of LTCs in MSNs decreases membrane excitability [10]. MSN activity produces the only output from the striatum and thus the finely tuned regulation of MSN activity is critical for normal motor function. Disruption of MSN regulation results in severe malfunction of the basal ganglia, as seen when MSNs lose dopaminergic input in Parkinson's disease, or when MSNs undergo cell death as seen in Huntington's disease [5, 44].

Because studying Ca²⁺ currents in MSNs has been challenging, we searched for a cell line that might serve as a model system for MSNs. However, remarkably few neuronal cell lines have been developed despite ongoing demand for their use in biophysical studies of ion channels and in high throughput systems for therapeutic drug testing. We hypothesized that ST14A cells, compared to HEK 293 cells, would express postsynaptic endogenous D₂R signaling microdomains closely matching MSNs, thus making ST14A cells useful for studying Ca_v1.3 modulation by D₂R specific signaling. Therefore we examined ST14A cells to determine whether this cell line exhibits sufficient striatal properties to serve as a suitable model system for studying MSN functioning. We first tested whether ST14A cells express endogenous voltage-gated Ca²⁺ current.

We characterized a small, endogenous Ca²⁺ current from differentiated ST14A cells that develop neuronal-like processes when grown at 37°C. However, we found that only 5/15 cells had a current amplitude larger than 200 pA even in the presence of the LTC agonist FPL. This small current and the relatively low number of cells expressing a measurable current, is similar to previous findings [29]. K⁺, Na⁺ and HCN-mediated currents, in addition to the ability to fire action potentials, are also reported in a small percentage of ST14A cells [29, 45, 46]. However, when present, the Ca²⁺ current was within the lower range of current amplitudes recorded in MSNs, and was similar to L-current in MSNs in that the tail current was sensitive to LTC agonists, increasing ~ 6-fold following exposure to FPL. L-current dominates few types of neurons; one of them being MSNs (e.g., [10] [47]). Though the Ca²⁺ current in differentiated ST14A cells is small, L-current appears to make up much of the whole-cell Ca²⁺ current. Further optimization of culture conditions and/or recording conditions may increase Ca_v1.3 expression and consequently L-current amplitudes.

As an alternative strategy to examining native Ca_v1.3 activity in ST14A cells, we attempted to transiently transfect round ST14A cells, which lack endogenous Ca²⁺ currents, with LTC channel subunits and GFP. We didn't know whether ST14A cells would tolerate transfection of the multiple Ca²⁺ channel subunits as well as express functional channels. However ST14A cells were transfected successfully with channel subunits and exhibited robust voltage-gated Ca²⁺ currents. We characterized the biophysical properties of isolated, recombinant Ca_v1.3 current in a striatal-like background without the complications of primary MSNs, i.e., requiring several pharmacological blockers to silence other ionic or multiple types of Ca²⁺ currents. These large currents appeared ideal for testing whether ST14A cells would support Ca_v1.3 current inhibition by the D₂R agonist.

From the biochemical characterization of ST14A cells as MSN-like due to the expression of dopamine receptors (D₁, D₂, D₄, D₅) and GAD65/67 mRNAs as well as expression of D₂R, M₁R, G_qα, cPLA₂ and PP2B protein we anticipated observing LTC modulation. However, no inhibition of Ca_v1.3 current was observed with Quin or Oxo-M. Since PLCβ-1 expression is so widespread, we tested for its expression in ST14A cells only after finding no LTC modulation by Quin. Lack of PLCβ-1 protein expression was unexpected since several intact signaling cascades are described in the growing literature regarding ST14A cells. Most notably, ST14A cells have functional CREB phosphorylation following D₂R stimulation and Ras/MAPK, adenylyl cyclase, Wnt and JAK/STAT signaling pathways [29, 48–51]. Moreover these cells express other enzymes that act on lipids including N-acyl-phosphatidylethanolamine-hydrolyzing phospholipase D (NAPE-PLD), fatty acid amide hydrolase, diacylglyceride lipase, monoacylglycerol lipase (Bari et al., 2013), and cPLA₂ (Fig 3C).

The absence of PLC β -1 expression in ST14A cells coincides with the lack of Ca_V1.3 current inhibition by either Quin or Oxo-M, supporting the importance of PLC β -1 for both D₂R and M₁R signal transduction pathways [10, 52, 53]. Despite PLC β -1's absence, it was not obvious that no other variant of PLC β would substitute for the missing PLC β -1. The absence of PLC β -1 and its apparent requirement for D₂R signaling will be of interest to researchers who study MSNs. Interestingly, PLC β -1 has been implicated in regulating growth and proliferation, where its absence results in uncontrolled cell proliferation [54, 55]. Thus a loss of PLC β -1 may have occurred during the immortalization of ST14A cells.

In these experiments, we used a short splice variant of Ca_V1.3, Ca_V1.3b [30]. Ca_V1.3a, which has a longer C-terminus, was not inhibited by activation of D₂Rs when expressed in HEK 293 cells [56]; however, Ca_V1.3a has been shown to bind the scaffolding protein Shank found in the postsynaptic density of synapses [57]. This association is necessary for Ca_V1.3 current inhibition by D₂Rs in primary MSNs [11]. Although the lack of the long C-terminus also could explain the absence of channel modulation by D₂Rs in ST14A cells, Ca_V1.3b LTCs can be modulated by both IGF-1 and AA. Exposure of SH-SY5Y cells expressing either Ca_V1.3a or Ca_V1.3b to IGF-1 enhances both currents and requires phosphorylation of S1486, a residue shared by both splice variants [58]. We have measured significant Ca_V1.3b inhibition by AA in transiently transfected HEK 293 cells, consistent with a potential transmembrane site of action [27].

Since AA release occurs in the striatum from both neurons and astrocytes [59–61] following stimulation of D₂Rs [21] or M₁Rs [62], we tested whether bath application of AA modulated LTC in ST14A cells to be certain that Ca_V1.3b could be modulated by molecules downstream of PLC β -1. We were unsure whether AA would inhibit Ca_V1.3b channels in ST14A cells similarly to Ca_V1.3 channels in HEK 293 cells [27] or native LTCs in SCG neurons [23–25] since a wide range of actions have been reported for AA modulation of a variety of Ca²⁺ currents by other groups (see review by Roberts-Crowley et al [63]). We found that direct application of AA circumvented the lack of receptor-activated channel modulation in ST14A cells and inhibited Ca_V1.3b recombinant current. This finding demonstrates that Ca_V1.3 channels are capable of being modulated in ST14A cells as we have observed previously in HEK 293 cells [27]. The properties of Ca_V1.3 inhibition by AA in HEK 293 and ST14A cells appear similar. Additionally we have found that Oxo-M inhibits currents from Ca_V1.3b in HEK 293 cells stably transfected with M₁Rs (unpublished data). Lastly, we have found that activation of D₂Rs by 10 μ M Quin inhibits Ca_V2.2 currents in HEK 293 cells (unpublished data) demonstrating that this agonist protocol should be sufficient to activate D₂Rs in ST14A cells. Therefore, the lack of current modulation by D₂Rs or M₁Rs, reported here, is supported by the absence of PLC β -1 rather than an inability of Ca_V1.3b to respond to modulation.

Conclusions

ST14A cells are used as a model system for both the study and treatment of Huntington's disease [64–69]. Despite the lack of D₂R- or M₁R-mediated Ca²⁺ channel modulation in ST14A cells reported here, this cell line was useful for elucidating that AA inhibits Ca_V1.3 channels. We hypothesize that the consistency of AA's inhibitory actions on Ca_V1.3 across cell types will be of interest to researchers who study lipid signaling molecules. Moreover, we anticipate the D₂R signaling cascade could be rescued by transfecting ST14A cells with PLC β -1. Whether D₂R signaling would then cause a lipid mediated inhibition of Ca_V1.3b LTCs awaits future studies. Thus, ST14A cells are a valuable tool for studying the biophysical properties of an isolated Ca²⁺ current and the modulation of these channels by signaling molecules within the context of a striatal background to aid in understanding neuronal malfunctions of the striatum.

Acknowledgments

We thank Michelle Ehrlich and Dr. Elena Cattaneo (Università degli Studi di Milano) for the ST14A cell line, Diane Lipscombe (Brown University) and Edward Perez-Reyes (University of Virginia) for channel cDNAs, Loretta Lee and TzuFeng (Annie) Chung of the UMASS Tissue Culture Facility for maintaining the ST14A, A9L and HEK 293 cells, and Maggie Lee for technical assistance. We also thank Rubing Zhao-Shea and John Heneghan for useful comments and Liwang Liu and Tora Mitra-Ganguli for review of the manuscript.

Author Contributions

Conceived and designed the experiments: MLR ARR. Performed the experiments: MLR. Analyzed the data: MLR. Contributed reagents/materials/analysis tools: ARR. Wrote the paper: MLR ARR.

References

1. Ahljianian MK, Westenbroek RE, Catterall WA. Subunit structure and localization of dihydropyridine-sensitive calcium channels in mammalian brain, spinal cord, and retina. *Neuron*. 1990; 4(6):819–32. PMID: [2163262](#).
2. Hirota K, Lambert DG. A comparative study of L-type voltage sensitive Ca²⁺ channels in rat brain regions and cultured neuronal cells. *Neurosci Lett*. 1997; 223(3):169–72. PMID: [9080459](#).
3. Catterall WA, Perez-Reyes E, Snutch TP, Striessnig J. International Union of Pharmacology. XLVIII. Nomenclature and structure-function relationships of voltage-gated calcium channels. *Pharmacol Rev*. 2005; 57(4):411–25. PMID: [16382099](#).
4. Nicola SM, Surmeier J, Malenka RC. Dopaminergic modulation of neuronal excitability in the striatum and nucleus accumbens. *Annu Rev Neurosci*. 2000; 23:185–215. PMID: [10845063](#).
5. Ehrlich ME. Huntington's disease and the striatal medium spiny neuron: cell-autonomous and non-cell-autonomous mechanisms of disease. *Neurotherapeutics: the Journal of the American Society for Experimental NeuroTherapeutics*. 2012; 9(2):270–84. doi: [10.1007/s13311-012-0112-2](#) PMID: [22441874](#); PubMed Central PMCID: PMC3337013.
6. Gerfen CR, Surmeier DJ. Modulation of striatal projection systems by dopamine. *Annu Rev Neurosci*. 2011; 34:441–66. doi: [10.1146/annurev-neuro-061010-113641](#) PMID: [21469956](#); PubMed Central PMCID: PMC3487690.
7. Hernandez-Lopez S, Bargas J, Surmeier DJ, Reyes A, Galarraga E. D1 receptor activation enhances evoked discharge in neostriatal medium spiny neurons by modulating an L-type Ca²⁺ conductance. *J Neurosci*. 1997; 17(9):3334–42. PMID: [9096166](#).
8. Surmeier DJ, Bargas J, Hemmings HC Jr., Nairn AC, Greengard P. Modulation of calcium currents by a D1 dopaminergic protein kinase/phosphatase cascade in rat neostriatal neurons. *Neuron*. 1995; 14(2):385–97. PMID: [7531987](#).
9. Missale C, Nash SR, Robinson SW, Jaber M, Caron MG. Dopamine receptors: from structure to function. *Physiological Reviews*. 1998; 78(1):189–225. PMID: [9457173](#).
10. Hernandez-Lopez S, Tkatch T, Perez-Garci E, Galarraga E, Bargas J, Hamm H, et al. D2 dopamine receptors in striatal medium spiny neurons reduce L-type Ca²⁺ currents and excitability via a novel PLC [beta]1-IP3-calcineurin-signaling cascade. *J Neurosci*. 2000; 20(24):8987–95. PMID: [11124974](#).
11. Olson PA, Tkatch T, Hernandez-Lopez S, Ulrich S, Ilijic E, Mugnaini E, et al. G-protein-coupled receptor modulation of striatal Ca_v1.3 L-type Ca²⁺ channels is dependent on a Shank-binding domain. *J Neurosci*. 2005; 25(5):1050–62. PMID: [15689540](#).
12. Mink JW. Neurobiology of basal ganglia circuits in Tourette syndrome: faulty inhibition of unwanted motor patterns? *Adv Neurol*. 2001; 85:113–22. PMID: [11530421](#).
13. Levant B. Novel drug interactions at D₂ dopamine receptors: modulation of [³H]quinpirole binding by monoamine oxidase inhibitors. *Life Sciences*. 2002; 71(23):2691–700. PMID: [12383877](#).
14. Ilijic E, Guzman JN, Surmeier DJ. The L-type channel antagonist isradipine is neuroprotective in a mouse model of Parkinson's disease. *Neurobiology of Disease*. 2011; 43(2):364–71. doi: [10.1016/j.nbd.2011.04.007](#) PMID: [21515375](#); PubMed Central PMCID: PMC3235730.
15. Kang S, Cooper G, Dunne SF, Dusel B, Luan CH, Surmeier DJ, et al. Ca_v1.3-selective L-type calcium channel antagonists as potential new therapeutics for Parkinson's disease. *Nature Communications*. 2012; 3:1146. doi: [10.1038/ncomms2149](#) PMID: [23093183](#).

16. Day M, Wang Z, Ding J, An X, Ingham CA, Shering AF, et al. Selective elimination of glutamatergic synapses on striatopallidal neurons in Parkinson disease models. *Nature Neuroscience*. 2006; 9(2):251–9. PMID: [16415865](#).
17. Basselin M, Chang L, Chen M, Bell JM, Rapoport SI. Chronic carbamazepine administration attenuates dopamine D₂-like receptor-initiated signaling via arachidonic acid in rat brain. *Neurochemical Research*. 2008; 33(7):1373–83. doi: [10.1007/s11064-008-9595-y](#) PMID: [18302021](#).
18. Bhattacharjee AK, Meister LM, Chang L, Bazinet RP, White L, Rapoport SI. In vivo imaging of disturbed pre- and post-synaptic dopaminergic signaling via arachidonic acid in a rat model of Parkinson's disease. *NeuroImage*. 2007; 37(4):1112–21. doi: [10.1016/j.neuroimage.2007.06.012](#) PMID: [17681816](#); PubMed Central PMCID: PMC2040339.
19. Bhattacharjee AK, Chang L, White L, Bazinet RP, Rapoport SI. D-Amphetamine stimulates D₂ dopamine receptor-mediated brain signaling involving arachidonic acid in unanesthetized rats. *Journal of cerebral blood flow and metabolism: official journal of the International Society of Cerebral Blood Flow and Metabolism*. 2006; 26(11):1378–88. doi: [10.1038/sj.jcbfm.9600290](#) PMID: [16511499](#).
20. Bhattacharjee AK, Chang L, Lee HJ, Bazinet RP, Seemann R, Rapoport SI. D₂ but not D₁ dopamine receptor stimulation augments brain signaling involving arachidonic acid in unanesthetized rats. *Psychopharmacology*. 2005; 180(4):735–42. doi: [10.1007/s00213-005-2208-4](#) PMID: [16163535](#).
21. Schinelli S, Paolillo M, Corona GL. Opposing actions of D₁- and D₂-dopamine receptors on arachidonic acid release and cyclic AMP production in striatal neurons. *J Neurochem*. 1994; 62(3):944–9. PMID: [8113815](#).
22. Kanterman RY, Mahan LC, Briley EM, Monsma FJ Jr., Sibley DR, Axelrod J, et al. Transfected D₂ dopamine receptors mediate the potentiation of arachidonic acid release in Chinese hamster ovary cells. *Molecular Pharmacology*. 1991; 39(3):364–9. PMID: [1848657](#).
23. Liu L, Barrett CF, Rittenhouse AR. Arachidonic acid both inhibits and enhances whole cell calcium currents in rat sympathetic neurons. *American Journal of Physiology Cell Physiology*. 2001; 280(5): C1293–305. PMID: [11287343](#).
24. Liu L, Rittenhouse AR. Effects of arachidonic acid on unitary calcium currents in rat sympathetic neurons. *J Physiol*. 2000; 525 Pt 2:391–404. PMID: [10835042](#); PubMed Central PMCID: PMC2269949.
25. Liu L, Zhao R, Bai Y, Stanish LF, Evans JE, Sanderson MJ, et al. M₁ muscarinic receptors inhibit L-type Ca²⁺ current and M-current by divergent signal transduction cascades. *J Neurosci*. 2006; 26(45):11588–98. doi: [10.1523/JNEUROSCI.2102-06.2006](#) PMID: [17093080](#).
26. Lin Z, Harris C, Lipscombe D. The molecular identity of Ca channel 1-subunits expressed in rat sympathetic neurons. *Journal of Molecular Neuroscience: MN*. 1996; 7(4):257–67. PMID: [8968947](#).
27. Roberts-Crowley ML, Rittenhouse AR. Arachidonic acid inhibition of L-type calcium (Ca_v1.3b) channels varies with accessory Ca_vβ subunits. *J Gen Physiol*. 2009; 133(4):387–403. doi: [10.1085/jgp.200810047](#) PMID: [19332620](#); PubMed Central PMCID: PMC2699108.
28. Cattaneo E, Conti L. Generation and characterization of embryonic striatal conditionally immortalized ST14A cells. *Journal of Neuroscience Research*. 1998; 53(2):223–34. PMID: [9671979](#).
29. Ehrlich ME, Conti L, Toselli M, Taglietti L, Fiorillo E, Taglietti V, et al. ST14A cells have properties of a medium-size spiny neuron. *Experimental Neurology*. 2001; 167(2):215–26. PMID: [11161610](#).
30. Xu W, Lipscombe D. Neuronal Ca_v1.3, L-type channels activate at relatively hyperpolarized membrane potentials and are incompletely inhibited by dihydropyridines. *J Neurosci*. 2001; 21(16):5944–51. Epub 2001/08/07. PMID: [11487617](#).
31. Surmeier DJ, Song WJ, Yan Z. Coordinated expression of dopamine receptors in neostriatal medium spiny neurons. *J Neurosci*. 1996; 16(20):6579–91. PMID: [8815934](#).
32. Kuppens E, Sabolek M, Anders U, Pilgrim C, Beyer C. Developmental regulation of glutamic acid decarboxylase mRNA expression and splicing in the rat striatum by dopamine. *Brain Research Molecular Brain Research*. 2000; 81(1–2):19–28. PMID: [11000475](#).
33. Torres JM, Gomez-Capilla JA, Ruiz E, Ortega E. Semiquantitative RT-PCR method coupled to capillary electrophoresis to study 5α-reductase mRNA isozymes in rat ventral prostate in different androgen status. *Mol Cell Biochem*. 2003; 250(1–2):125–30. PMID: [12962150](#).
34. Liu L, Roberts ML, Rittenhouse AR. Phospholipid metabolism is required for M₁ muscarinic inhibition of N-type calcium current in sympathetic neurons. *European Biophysics Journal: EBJ*. 2004; 33(3):255–64. doi: [10.1007/s00249-003-0387-7](#) PMID: [15004729](#).
35. Yue DT, Backx PH, Imredy JP. Calcium-sensitive inactivation in the gating of single calcium channels. *Science*. 1990; 250(4988):1735–8. PMID: [2176745](#).
36. Chien AJ, Carr KM, Shirokov RE, Rios E, Hosey MM. Identification of palmitoylation sites within the L-type calcium channel β_{2a} subunit and effects on channel function. *The Journal of Biological Chemistry*. 1996; 271(43):26465–8. PMID: [8900112](#).

37. Yan Z, Flores-Hernandez J, Surmeier DJ. Coordinated expression of muscarinic receptor messenger RNAs in striatal medium spiny neurons. *Neuroscience*. 2001; 103(4):1017–24. PMID: [11301208](#).
38. Moreland RB, Nakane M, Donnelly-Roberts DL, Miller LN, Chang R, Uchic ME, et al. Comparative pharmacology of human dopamine D₂-like receptor stable cell lines coupled to calcium flux through G_{qo5}. *Biochem Pharmacol*. 2004; 68(4):761–72. PMID: [15276084](#).
39. Bitner RS, Nikkel AL, Otte S, Martino B, Barlow EH, Bhatia P, et al. Dopamine D₄ receptor signaling in the rat paraventricular hypothalamic nucleus: Evidence of natural coupling involving immediate early gene induction and mitogen activated protein kinase phosphorylation. *Neuropharmacology*. 2006; 50(5):521–31. PMID: [16324724](#).
40. Ahlgren-Beckendorf JA, Levant B. Signaling mechanisms of the D₃ dopamine receptor. *J Recept Signal Transduct Res*. 2004; 24(3):117–30. PMID: [15521358](#).
41. Fishburn CS, Elazar Z, Fuchs S. Differential glycosylation and intracellular trafficking for the long and short isoforms of the D₂ dopamine receptor. *The Journal of Biological Chemistry*. 1995; 270(50):29819–24. PMID: [8530376](#).
42. Lin JY, Chung KK, de Castro D, Funk GD, Lipski J. Effects of muscarinic acetylcholine receptor activation on membrane currents and intracellular messengers in medium spiny neurones of the rat striatum. *Eur J Neurosci*. 2004; 20(5):1219–30. PMID: [15341594](#).
43. Spector AA. Fatty acid binding to plasma albumin. *Journal of Lipid Research*. 1975; 16(3):165–79. PMID: [236351](#).
44. Herrero MT, Barcia C, Navarro JM. Functional anatomy of thalamus and basal ganglia. *Childs Nerv Syst*. 2002; 18(8):386–404. PMID: [12192499](#).
45. Strauss U, Bajorat R, Mueller J, Rolfs A, editors. "Hidden" Sodium Currents in Neuronal Progenitor Cells. 2003: Washington, DC: Society for Neuroscience, Online.
46. Bajorat R, Brauer AU, Wasner U, Rolfs A, Strauss U. Functional significance of HCN2/3-mediated I(h) in striatal cells at early developmental stages. *Journal of Neuroscience Research*. 2005; 82(2):206–13. PMID: [16175581](#).
47. Martella G, Madeo G, Schirinzi T, Tassone A, Sciamanna G, Spadoni F, et al. Altered profile and D₂-dopamine receptor modulation of high voltage-activated calcium current in striatal medium spiny neurons from animal models of Parkinson's disease. *Neuroscience*. 2011; 177:240–51. doi: [10.1016/j.neuroscience.2010.12.057](#) PMID: [21195752](#).
48. Varani K, Rigamonti D, Sipione S, Camurri A, Borea PA, Cattabeni F, et al. Aberrant amplification of A_{2A} receptor signaling in striatal cells expressing mutant huntingtin. *FASEB journal: official publication of the Federation of American Societies for Experimental Biology*. 2001; 15(7):1245–7. PMID: [11344102](#).
49. Bottcher T, Mix E, Koczan D, Bauer P, Pahnke J, Peters S, et al. Gene expression profiling of ciliary neurotrophic factor-overexpressing rat striatal progenitor cells (ST14A) indicates improved stress response during the early stage of differentiation. *Journal of Neuroscience Research*. 2003; 73(1):42–53. PMID: [12815707](#).
50. Cattaneo E, De Fraja C, Conti L, Reinach B, Bolis L, Govoni S, et al. Activation of the JAK/STAT pathway leads to proliferation of ST14A central nervous system progenitor cells. *The Journal of Biological Chemistry*. 1996; 271(38):23374–9. PMID: [8798541](#).
51. Lange C, Mix E, Rateitschak K, Rolfs A. Wnt signal pathways and neural stem cell differentiation. *Neurodegener Dis*. 2006; 3(1–2):76–86. PMID: [16909041](#).
52. Wu L, Bauer CS, Zhen XG, Xie C, Yang J. Dual regulation of voltage-gated calcium channels by PtdIns(4,5)P₂. *Nature*. 2002; 419(6910):947–52. PMID: [12410316](#).
53. Liu L, Rittenhouse AR. Arachidonic acid mediates muscarinic inhibition and enhancement of N-type Ca²⁺ current in sympathetic neurons. *Proceedings of the National Academy of Sciences of the United States of America*. 2003; 100(1):295–300. doi: [10.1073/pnas.0136826100](#) PMID: [12496347](#); PubMed Central PMCID: PMC140955.
54. Cocco L, Follo MY, Faenza I, Billi AM, Ramazzotti G, Martelli AM, et al. Inositol signaling in the nucleus: from physiology to pathology. *Advances in Enzyme Regulation*. 2010; 50(1):2–11. Epub 2009/11/10. doi: [10.1016/j.advenzreg.2009.10.007](#) PMID: [19895834](#).
55. Cocco L, Follo MY, Faenza I, Fiume R, Ramazzotti G, Weber G, et al. Physiology and pathology of nuclear phospholipase C beta1. *Advances in Enzyme Regulation*. 2011; 51(1):2–12. Epub 2010/11/03. doi: [10.1016/j.advenzreg.2010.09.015](#) PMID: [21035488](#).
56. Bell DC, Butcher AJ, Berrow NS, Page KM, Brust PF, Nesterova A, et al. Biophysical properties, pharmacology, and modulation of human, neuronal L-type (1D, Ca_v1.3) voltage-dependent calcium currents. *Journal of Neurophysiology*. 2001; 85(2):816–27. PMID: [11160515](#).

57. Zhang H, Maximov A, Fu Y, Xu F, Tang TS, Tkatch T, et al. Association of Ca_v1.3 L-type calcium channels with Shank. *J Neurosci*. 2005; 25(5):1037–49. doi: [10.1523/JNEUROSCI.4554-04.2005](https://doi.org/10.1523/JNEUROSCI.4554-04.2005) PMID: [15689539](https://pubmed.ncbi.nlm.nih.gov/15689539/).
58. Gao L, Blair LA, Salinas GD, Needleman LA, Marshall J. Insulin-like growth factor-1 modulation of Ca_v1.3 calcium channels depends on Ca²⁺ release from IP₃-sensitive stores and calcium/calmodulin kinase II phosphorylation of the 1 subunit EF hand. *J Neurosci*. 2006; 26(23):6259–68. Epub 2006/06/10. doi: [10.1523/jneurosci.0481-06.2006](https://doi.org/10.1523/jneurosci.0481-06.2006) PMID: [16763033](https://pubmed.ncbi.nlm.nih.gov/16763033/).
59. Zanassi P, Paolillo M, Schinelli S. Coexpression of phospholipase A₂ isoforms in rat striatal astrocytes. *Neurosci Lett*. 1998; 247(2–3):83–6. PMID: [9655598](https://pubmed.ncbi.nlm.nih.gov/9655598/).
60. Rouach N, Tence M, Glowinski J, Giaume C. Costimulation of N-methyl-D-aspartate and muscarinic neuronal receptors modulates gap junctional communication in striatal astrocytes. *Proceedings of the National Academy of Sciences of the United States of America*. 2002; 99(2):1023–8. PMID: [11792837](https://pubmed.ncbi.nlm.nih.gov/11792837/).
61. Blanchet F, Gauchy C, Perez S, Glowinski J, Kemel ML. Role of arachidonic acid in the regulation of the NMDA-evoked release of acetylcholine in striatal compartments. *Synapse*. 1999; 31(2):140–50. PMID: [10024011](https://pubmed.ncbi.nlm.nih.gov/10024011/).
62. Tence M, Cordier J, Premont J, Glowinski J. Muscarinic cholinergic agonists stimulate arachidonic acid release from mouse striatal neurons in primary culture. *The Journal of Pharmacology and Experimental Therapeutics*. 1994; 269(2):646–53. PMID: [8182531](https://pubmed.ncbi.nlm.nih.gov/8182531/).
63. Roberts-Crowley ML, Mitra-Ganguli T, Liu L, Rittenhouse AR. Regulation of voltage-gated Ca²⁺ channels by lipids. *Cell Calcium*. 2009; 45(6):589–601. doi: [10.1016/j.ceca.2009.03.015](https://doi.org/10.1016/j.ceca.2009.03.015) PMID: [19419761](https://pubmed.ncbi.nlm.nih.gov/19419761/); PubMed Central PMCID: PMC2964877.
64. Weinelt S, Peters S, Bauer P, Mix E, Haas SJ, Dittmann A, et al. Ciliary neurotrophic factor overexpression in neural progenitor cells (ST14A) increases proliferation, metabolic activity, and resistance to stress during differentiation. *Journal of Neuroscience Research*. 2003; 71(2):228–36. PMID: [12503085](https://pubmed.ncbi.nlm.nih.gov/12503085/).
65. Rigamonti D, Bauer JH, De-Fraja C, Conti L, Sipione S, Sciorati C, et al. Wild-type huntingtin protects from apoptosis upstream of caspase-3. *J Neurosci*. 2000; 20(10):3705–13. PMID: [10804212](https://pubmed.ncbi.nlm.nih.gov/10804212/).
66. Zuccato C, Tartari M, Crotti A, Goffredo D, Valenza M, Conti L, et al. Huntingtin interacts with REST/NRSF to modulate the transcription of NRSE-controlled neuronal genes. *Nat Genet*. 2003; 35(1):76–83. PMID: [12881722](https://pubmed.ncbi.nlm.nih.gov/12881722/).
67. Bosch M, Pineda JR, Sunol C, Petriz J, Cattaneo E, Alberch J, et al. Induction of GABAergic phenotype in a neural stem cell line for transplantation in an excitotoxic model of Huntington's disease. *Experimental Neurology*. 2004; 190(1):42–58. PMID: [15473979](https://pubmed.ncbi.nlm.nih.gov/15473979/).
68. Bari M, Battista N, Valenza M, Mastrangelo N, Malaponti M, Catanzaro G, et al. In vitro and in vivo models of Huntington's disease show alterations in the endocannabinoid system. *The FEBS Journal*. 2013; 280(14):3376–88. doi: [10.1111/febs.12329](https://doi.org/10.1111/febs.12329) PMID: [23659592](https://pubmed.ncbi.nlm.nih.gov/23659592/).
69. Ermak G, Hench KJ, Chang KT, Sachdev S, Davies KJ. Regulator of calcineurin (RCAN1-1L) is deficient in Huntington disease and protective against mutant huntingtin toxicity in vitro. *The Journal of Biological Chemistry*. 2009; 284(18):1845–53. doi: [10.1074/jbc.M900639200](https://doi.org/10.1074/jbc.M900639200) PMID: [19270310](https://pubmed.ncbi.nlm.nih.gov/19270310/); PubMed Central PMCID: PMC2673253.